SURFACE MOUNT ASSEMBLY FAILURE STATISTICS AND FAILURE-FREE TIMES

by J-P. Clech, D. M. Noctor, J. C. Manock, G. W. Lynott and F. E. Bader
AT&T Bell Laboratories
[appeared in Proceedings, 44th ECTC, Washington, D.C., May 1-4, 1994, pp. 487-497]

ABSTRACT

This paper presents new and improved practices for the engineering analysis of Surface Mount (SM) attachment failure statistics. The concept of failure free times is introduced for SM assembly reliability assessment using a three parameter Weibull analysis of failure data. The failure free metric is similar to a warranty period during which thermo-mechanical fatigue failures of solder joints are not expected. Based on the correlation of a large test database, it is demonstrated that the Comprehensive Surface Mount Reliability (CSMR) model can predict failure-free times. The three parameter Weibull treatment provides more accurate reliability projections, potentially qualifying component assemblies that would be rated marginal or unacceptable based on conservative two parameter Weibull or log-normal analysis.

INTRODUCTION

Statistical analysis of solder joint failure data is an essential part of Surface Mount (SM) assembly reliability assessment programs. Assembly reliability is estimated by linear acceleration of the distribution of times-to-failure from test to use conditions and by the projection of accelerated test data of small sample sizes to low failure percentiles representative of cumulative failure probabilities required in the field. The accuracy of field reliability projections is strongly dependent on the choice of the underlying statistical distribution and on the assumed or estimated values of the parameters defining that distribution. This document reviews existing practices for statistical analysis of solder joint failure data and presents new and improved practices based on the analysis of an extensive set of failure data.

Tests of goodness-of-fit were run to assess the fit of thermo-mechanical wear out failure data from 26 accelerated tests to two and three parameter Weibull [1-6] and log-normal [4, 6] distributions. The three parameter (3P) Weibull distribution provides a better fit to the test data and more accurate projections at low failure percentiles where both the two parameter (2P) Weibull and the log-normal distributions are found to be conservative. The third parameter of the 3P Weibull distribution is the failure free time. The other two parameters are the characteristic life and the shape parameter as in the more commonly used 2P Weibull distribution. Failure free times scaled for solder crack areas correlate to cyclic inelastic strain energy as in the CSMR correlation of characteristic lives [7]. This additional feature of the CSMR model provides the capability to predict failure free times at the design stage. This enhancement of our modeling capability is expected to predict better field reliability, especially for SM components that were previously rated as marginal, and for emerging technologies and applications placing higher stresses on solder joints. Application examples are given including the use of the 3P Weibull distribution to predict failure-free times in a design application or to extrapolate accelerated test data to field conditions.

SOLDER JOINT FAILURE STATISTICS

Failure Definition

Solder joint failure data and the underlying statistical distributions are a function of the chosen failure definition. Throughout this document, solder joint failures are determined by the high

resistance of a continuously monitored test channel [8, 9]. For most datasets analyzed, an electrical failure is the first intermittent flagged by an Anatech™ [1] event detector as a 1000 ohm *in-situ* resistance reading of a 0.2 microsecond minimum duration across a test channel. Six older datasets used non *in-situ* resistance measurements as a failure criterion. This did not result in any noticeable discrepancy across our database as these test vehicles were leadless chip carriers that failed rather quickly. Solder joint failure statistics for other criteria such as crack initiation and percent of peripheral cracking [10] or strength degradation [11, 12] were not investigated in this study.

Infant Mortality

Solder joint failures are hypothesized to follow a bath-tub reliability curve [9] as shown in Figure 1. Infant mortality failures occur early in the life cycle and have decreasing failure rates while wear out failures have increasing failure rates. It is the intent of design-for-reliability practices that no significant wear out occurs during the product service life. Infant mortality failures need to be separated from the wear out failure distribution when analyzing life test data. Environmental stress testing [13] is used to screen poor quality assemblies that would be prone to infant mortality in service. Process control corrective measures ensure that SM assemblies that are shipped are of high enough quality and do not fail in the field until the wear out threshold is reached.

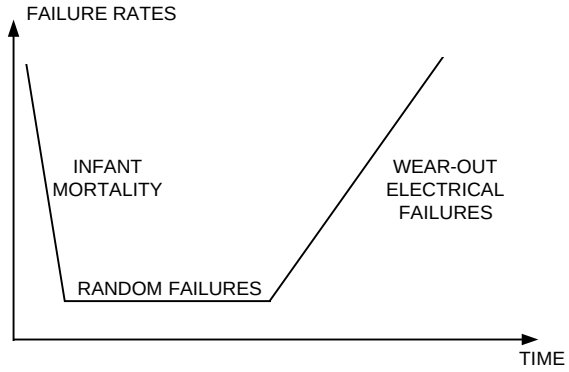

Figure 1: Bath-tub Reliability Curve.

An example of infant mortality data during the initial part of the bath-tub reliability curve is shown in Figure 2. 132 I/O PQFP (Plastic Quad Flat Pack) test vehicles repaired with a hot air reflow machine were thermally cycled between 0^{o}C and 100^{o}C at a frequency of 96 cycles/day. [14] Ten first device failures were recorded out of a total of 60 devices. The first failure was detected at 2 cycles, the last at 14615 cycles and no other failure occurred until the test was ended at 17,550 cycles. Failures were attributed to low solder volume on the leads that gave the first device electrical opens.

[1] Anatech™ is a trademark of the Anatech company.

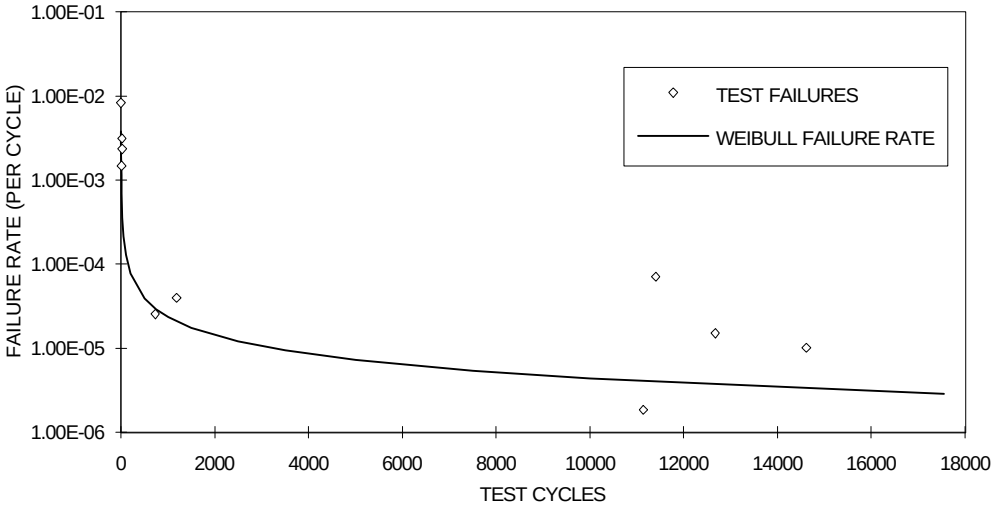

Figure 2: Device Attachment Infant Mortality Data with Decreasing Failure Rates.

The failure rate curve in Figure 2 is the instantaneous hazard rate function for the 2P Weibull distribution shown in Figure 3 [2]. The 2P Weibull distribution has a slope less than 1, dictating the decreasing failure rates characteristic of infant mortality data.

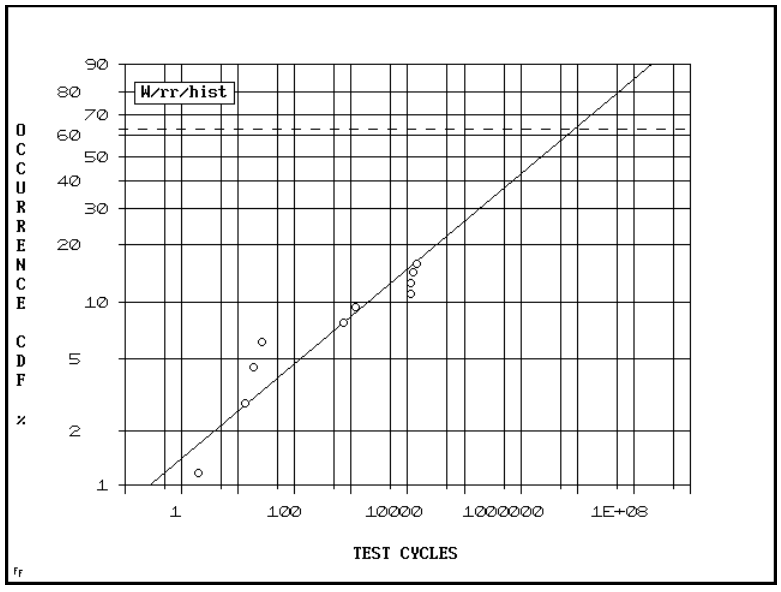

Figure 3: 2P Weibull Distribution of PQFP Infant Mortality Failures (slope: $\beta = 0.266$).

Accelerated Life Tests and Linear Acceleration

The rest of this document addresses the statistical analysis of wear out failure data. SM field reliability estimates obtained from accelerated life test data assume a constant Acceleration Factor (AF). AFs are obtained from physical models that relate times-to-failure to applied

[2] Log-normal and Weibull plots in this document were generated by the WeibullSMITH™ software. WeibullSMITH™ is a trademark of the Fulton Findings company.

"stresses" for specific failure modes, solder compositions and assembly technologies. Acceleration models have been developed, for example, for 95Pb-5Sn and 97Pb-3Sn flip-chip attachment [15, 16] and eutectic or near-eutectic Sn-Pb SM assemblies [7, 11, 17-21]. AFs are a time compression factor [6] that give the failure distribution in service by shifting the failure distribution of test data to field conditions as shown in Figure 4.

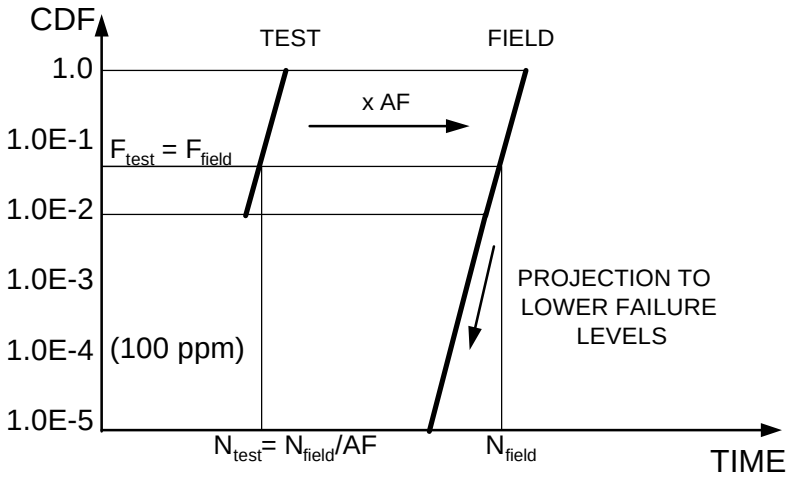

Figure 4: Linear Acceleration of Test Wear-Out Data and Projection to Lower Failure Levels Required in the Field.

For linear acceleration, the relationship between the Cumulative Distribution of Failures (CDF) functions F_{field} and F_{test} for field and test conditions is (see Figure 4):

$$F_{field}(N_{field}) = F_{test}(\frac{N_{field}}{AF}) \quad (1)$$

where N_{field} is a random time or cycles to failure under field conditions. The field service life $N_{field}(F)$ for a required CDF of F is:

$$N_{field}(F) = AF \times N_{test}(F) \quad (2)$$

where $N_{test}(F)$ is the equivalent test time under accelerated test conditions for the same cumulative failure level F at time $N_{field}(F)$ in the field. Equations (1) and (2) are equivalent and hold regardless of the underlying statistical distribution.

Figure 5 shows device attachment failure times for one stress condition versus another stress condition for three datasets [22, 23]. The data is from identical test vehicles (25 mil pitch leadless chip carriers on organic boards, 60Sn-40Pb solder) tested under three different thermal cycling conditions (30^oC to 130^oC, 30^oC to 70^oC and 30^oC to 90^oC) at a common frequency of 58 cycles/day. The three datasets plotted on a log-log scale are almost parallel to the ascending diagonal of the plot. This supports the assumption of linear acceleration without any presumption of the underlying statistical distribution. Life-test data from IBM also support the assumption of constant acceleration factors for flip-chip [16] and ceramic Ball Grid Array (BGA) [24] assembly reliability. In both cases (flip-chip and ceramic BGAs), failure data from mild and highly accelerated thermal cycling tests were found to follow parallel distributions on log-normal plots.

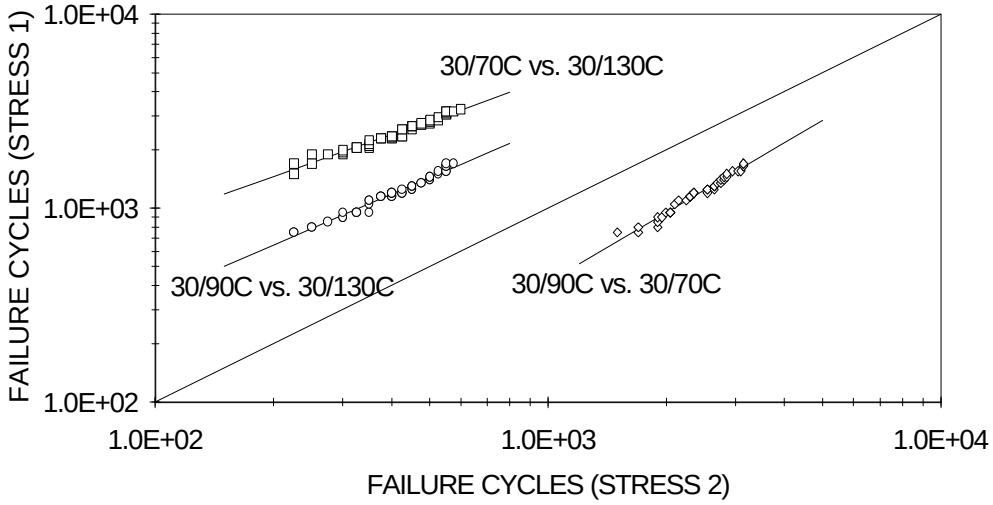

Figure 5: Verification of Linear Acceleration Assumption.

Statistical Failure Distributions

The next and perhaps most important issue with solder joint accelerated life test models is the choice of a statistical distribution of times-to-failure that fits the early part of the wear-out failure distribution well. The first wear-out failures under accelerated testing conditions are of most interest, much more so than median lives since we are concerned with low failure percentiles in the field. The required end of life CDF for assembly reliability in industrial telecommunication applications is typically less than 100 to 200 ppm (0.01% to 0.02%) on a component basis. For small test samples, the log-normal and 2P Weibull distributions may fit the failure data equally well over a limited range of high CDFs. However, their projections to the lower cumulative failure levels of interest may be very different as shown in the examples below. Sample sizes are less than 100 devices in general and CDFs for the test populations start at 1000 ppm or a few percent, that is, one to two orders of magnitude higher than a 100 ppm field requirement (Figure 4).

Figure 6 shows the fit of several statistical distributions to test failure data for a dataset with 190 devices. The solder joint cycles to failure are for ceramic resistor networks on organic circuit boards subjected to thermal cycling between 0^{o}C and 100^{o}C at a frequency of 72 cycles/day.[25]

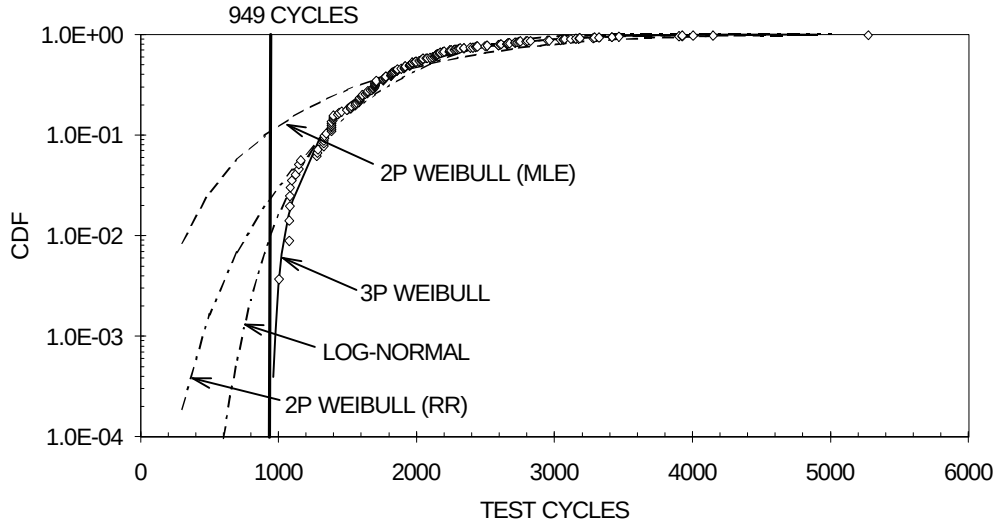

Figure 6: Ceramic Resistor Network Data: Fit of Statistical Failure Distributions to Test Cycles to Failure.

The 3P Weibull distribution shows the best overall fit. On the high end, the four distributions fit equally well and give approximately similar values of median lives. On the low end, the 2P Weibull with Maximum Likelihood Estimates (MLE) [3, 6] results in a conservative fit as it predicts a CDF of 10% at 909 cycles, that is, 19 devices are predicted to fail by 909 cycles. In the test, the first failure actually occurred at 1002 test cycles with an estimated CDF of 0.37% [3]. The 2P Weibull using a Rank-Regression (RR) [3, 6] algorithm provides a slightly better fit. The log-normal distribution provides the next best fit with 1% failure at 943 cycles. The 3P Weibull distribution is asymptotic to a vertical line at 949 cycles. This is interpreted as a minimum life or failure free time.

	Distribution			
CDF	2P Weibull (MLE)	2P Weibull (RR)	Log-Normal	3P Weibull
1%	324	768	943	1045
0.1%	118	445	737	975
0.01%	43	258	601	957

Table 1: Cycles to CDF's of 0.01%, 0.1% and 1% (from data in Figure 6).

Numbers of cycles to failure probabilities of 0.01%, 0.1% and 1% for the four distributions are given in Table 1. Figure 6 and Table 1 show the conservatism of 2P Weibull projections at lower failure levels. For example, a CDF of 0.1% occurs at 445 cycles on the 2P Weibull (RR) curve and at 975 cycles on the 3P Weibull curve. In terms of field life with a 0.1% CDF requirement, the 3P Weibull allows for a design life a factor of 975/445 = 2.19 times longer than the 2P Weibull. The 2.19 times difference is significant since it translates into, for example, limiting a design life to 10 years based on 2P Weibull or 21.9 years based on 3P Weibull analysis. This difference becomes larger at lower CDFs (e.g.: a factor of 957/258 = 3.7 for a CDF of 0.01%).

The downward deviation of the test data at the low end of the failure distributions shows similarly on 2P Weibull and log-normal plots when the sample size is large enough. The data in Figures

[3] The population CDFs at test failure times are calculated using the median rank algorithm recommended in Ref. 6 (p. 112). The preferred estimate of the CDF at the i^{th} failure for a starting sample size of n is: $F(i) = (i - 0.3) / (n + 0.4)$ for i = 1, 2, 3...

7, 8 and 9 is for SOT (Small Outline Transistor) components assembled on FR-4 circuit boards and tested under accelerated conditions between 0^{o}C and 100^{o}C at a frequency of 100 cycles/day [26]. The sample size was 120 components and failures were reported on a per component basis. The first failure occurred at 4650 cycles and 58 components, that is 48 % of the sample size, had not failed when the test was interrupted at 13589 cycles. The curvature of the data in Figures 7 and 8 suggests that a 3P Weibull distribution is a more appropriate distribution [1-5]. The data aligns on a 3P Weibull plot by shifting the origin of the time axis to the minimum life (Figure 9). The expected failure free time from the 3P Weibull analysis is 4465 cycles (Figure 9). Similar observations were made by E. Nicewarner [27, 28] on a large number of datasets showing that the 3P Weibull is a more accurate distribution for solder joint failure statistics.

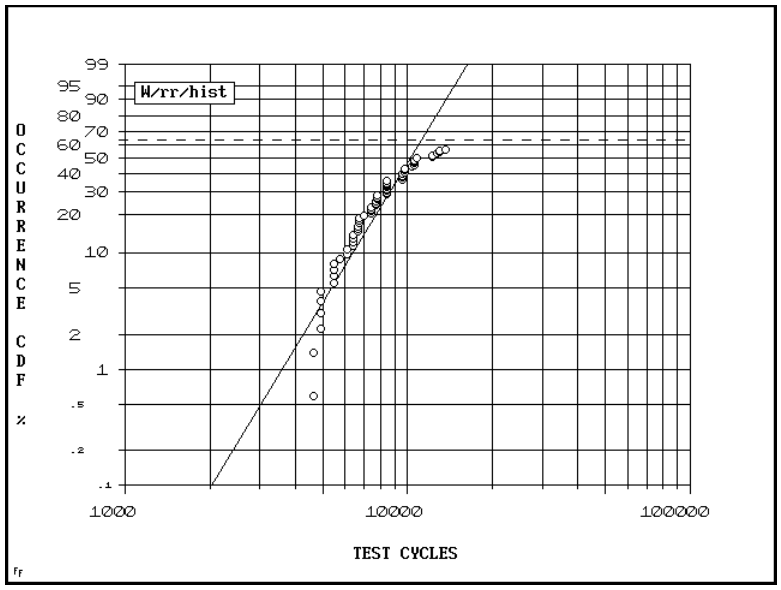

Figure 7: 2P Weibull Plot of SOT Failure Data.

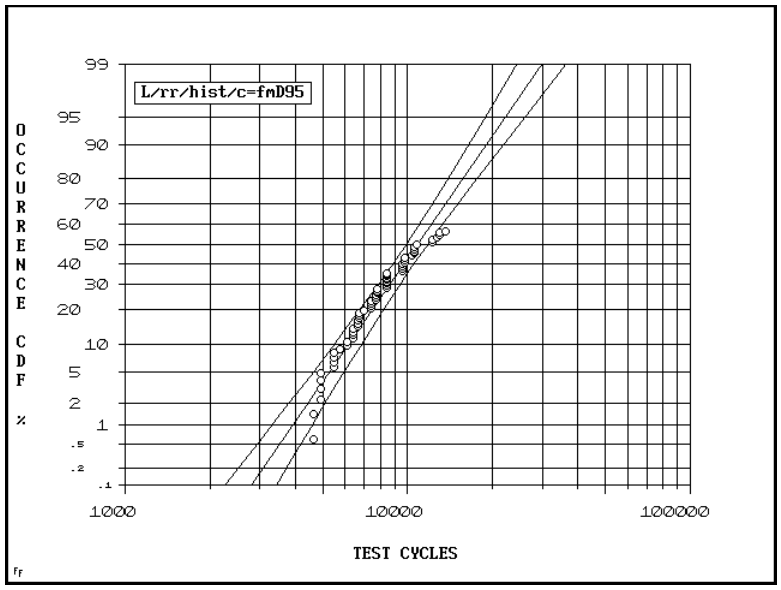

Figure 8: Log-Normal Plot of SOT Failure Data with 95% Confidence Bands.

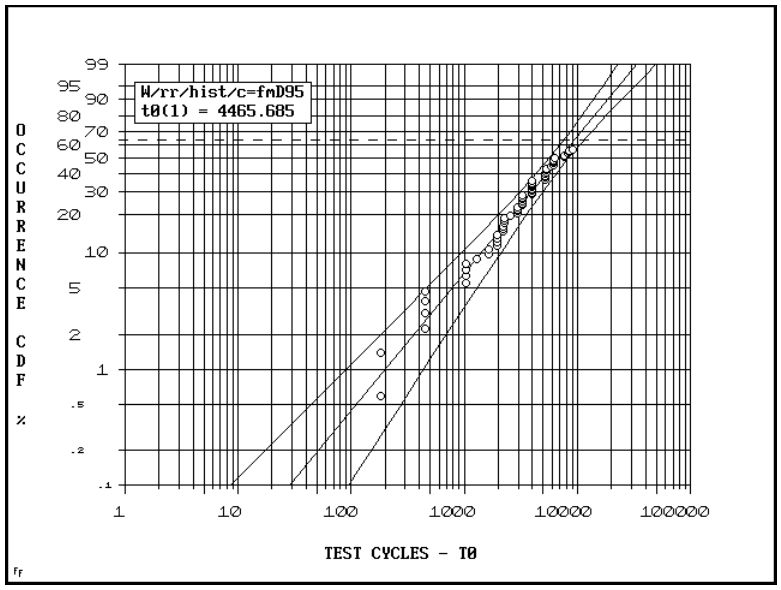

Figure 9: 3P Weibull Plot of SOT Failure Data with 95% Confidence Bands.

BEST WORKING DISTRIBUTION

Database Tests

Tests of goodness-of-fit of statistical distributions were run on 26 independent datasets that had complete failure logs available. The test vehicles covered a wide range of circuit board technologies and components including discretes, leadless and leaded perimeter packages and area array packages [7]. Solder composition was eutectic or near-eutectic tin-lead. For each dataset, failure statistics were fit to log-normal, 2P and 3P Weibull distributions as shown in Figures 7 to 9 for the SOT data. The correlation coefficients are shown in Figure 10 where the datasets are rank-ordered by increasing values of r^2 for the 2P Weibull (RR) distributions.

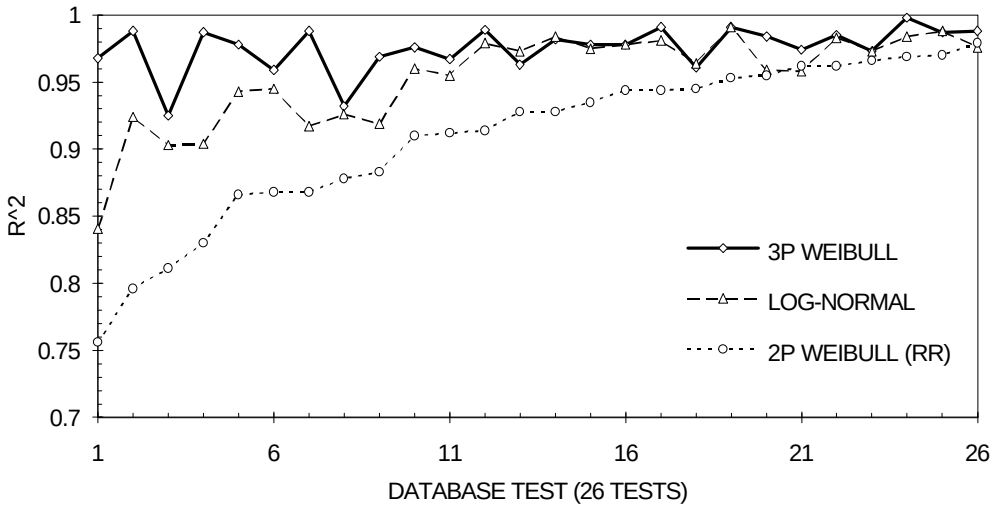

Figure 10: Database Correlation Coefficients for Log-Normal, 2P and 3P Weibull Distributions.

The correlation coefficients for the 3P Weibull distributions are larger than 0.95 except for two tests with r^2 values of 0.925 and 0.932. The correlation coefficients for the log-normal distributions of 9 datasets are less than 0.95 and as low as 0.84. The r^2 's for the 2P Weibull distributions of 18 datasets are less than 0.95 and as low as 0.75 for 18 datasets. Based on the results of these statistical tests, the 3P Weibull distribution appears to work best and is our preferred statistical distribution for the engineering analysis of solder joint failure data. The 3P Weibull distribution supersedes our previous use of 2P Weibull's.

Physical Interpretation

The log-normal distribution, which applies well to failure mechanisms encountered in semi-conductor reliability such as electro-migration, corrosion and other chemical processes [6, 29], appears as a competitor to the 3P Weibull, which is a preferred distribution for strength and fatigue of materials [5, 30-32]. However, the multiplicative degradation theory that leads to the log-normal distribution [6, 29] does not agree with constant crack propagation and strength degradation rates measured during thermal cycling of surface mount assemblies [21, 33, 34]. Using the crack area, A, as the random variable that describes the state of degradation in a solder joint at a given cycle, the crack area at the next cycle is $A + \Delta A$ where ΔA is the incremental crack growth per cycle. According to the log-normal theory [6, 29], the increase in degradation is proportional to the present state of degradation, that is: $\Delta A = k \times A$, where k is the degradation proportionality factor. The log-normal theory thus gives crack propagation rates that increase with the crack area during thermal cycling. This conflicts with measurements by R. Darveaux [21] who found that cracks in solder joints of area array packages grow at a constant rate during thermal cycling. Crack initiation was about 10% of the fatigue life and a linear relationship existed between crack length and thermal cycles for seven test conditions covering a wide range of temperature swings and cyclic frequencies. Similar observations were made by Y. Uegai et al. [33] for crack growth in solder joints of Alloy 42 leaded PQFPs. The constant crack propagation rate model agrees with the scaling of cyclic life for the solder crack area in the CSMR model [7]. The quantitative agreement between the two models is shown later in Figure 14. Using joint strength as another variable that describes solder joint degradation, J. Seyyedi et al. [12, 34] found that solder joint strength decreases linearly with increasing number of thermal cycles for several solder compositions including eutectic tin-lead. The degradation of strength at a constant rate does not support the log-normal theory either.

The Weibull distribution is an extreme or lowest value distribution derived from weakest link theory [1-6, 32]. In SM attachment reliability, we are concerned with component attachment failures defined as the first interconnect open among the weakest or highly stressed solder joints of a given component. For example, in assessing the attachment reliability of a 68 I/O peripheral component, failure statistics for the test population are times-to-failure of the worst joints where, for each component under test, the worst joint is the weakest of 68 joints, likely one of 8 corner joints, that fails first. Since our accelerated tests are analyzed and extrapolated on the basis of first device failures, our wear-out failure data are weakest link statistics that lend themselves well to an extreme value distribution like the Weibull distribution.

The interpretation of the minimum life that stems from the 3P Weibull distribution of solder joint electrical failures is as follows. While solder joint damage mechanisms are activated early during thermal cycling, wear-out failures do not occur until a critical damage level, or failure threshold, has been reached and cracks have propagated through the joints. Under thermal cycling conditions, wear-out failures are preceded by a sequence of microstructural coarsening and deformations due to plastic flow and creep, crack initiation and growth, and crack propagation or coalescence through the solder joints [35-38], all of which take time. A population of a given type of SM component with solder joints of acceptable quality is thus expected to remain electrically failure-free for a minimum amount of time, the assembly failure-free time. The weakest joint for the component population fails open when the deployed assemblies reach

the failure threshold. The more resilient joints fail at later times following a Weibull distribution which starts at the minimum life and whose shape parameter captures the spread of joint quality within the population. The distribution of failure times reflects joint-to-joint differences in solder volume, geometry, microstructures and micro-mechanical failure paths as well as differences in applied loads.

While we lack field data to test failure distributions under use conditions, to our knowledge, the large number of AT&T SM circuit packs that have been deployed in the field for the last 10 years or so are essentially free of solder joint wear-out failures. This supports the use of a failure distribution with a minimum life parameter. The main benefit of this enhanced treatment of SM failure data is that the 3P Weibull analysis allows for the qualification of component assemblies that would be rated marginal based on conservative 2P Weibull projections.

TEST DATA CORRELATION

The CDF for the 3P Weibull distribution is:

$$\text{for } N < N_0: \quad F(N) = 0 \qquad (3)$$

$$\text{for } N > N_0: \quad F(N) = 1 - \exp\left[-\left(\frac{N - N_0}{\alpha - N_0}\right)^{\beta}\right]$$

where the three independent parameters are:

- The minimum life or failure-free time, N_0, prior to which no failures are expected.
- The characteristic life, α, or time to a CDF of $1 - 1/e \approx 63.2\%$.
- The shape parameter, β, given by the slope of the failure distribution on Weibull paper with the origin of the time axis shifted to N_0.

Other useful equations and properties of the 3P Weibull distribution are given in Appendix.

We use the CSMR modeling approach to estimate α and N_0. The original CSMR correlation of characteristic lives [7] across our test database remains valid since test cycles to the 63.2% failure level are approximately the same whether the data is fit with 2P or 3P Weibull distributions. The CSMR predictive capability has been enhanced by correlating test failure-free times in a similar manner. Figures 11 and 12 show correlations of failure-free times and characteristic lives scaled for the solder crack area A (N_0/A and α/A, respectively) versus cyclic inelastic strain energy ΔW_{in} [8]. The regression lines have slopes close to -1. The median slopes are: -0.93 with 95% confidence bands: (-1.07, -0.78) for the N_0/A correlation; -1.05 with 95% confidence bands: (-1.17, -0.94) for the α/A correlation. The spread of the data is a factor of two times below and three times above the regression lines. Such a spread is typical of fatigue lives. [11, 39]

The shape parameter β ranges from 1 to 5.5 across our database with a median value of 2.2. The standard deviation of β across the database is 1.1. and the one standard deviation range for β is 1.1 to 3.3. The average value $\beta = 2.2$ compares with typical values of $\beta = 1.5$ and 2.0 for 3P Weibull distributions used in the bearings industry for the reliability of ball bearings and roller bearings respectively. [40, 41]

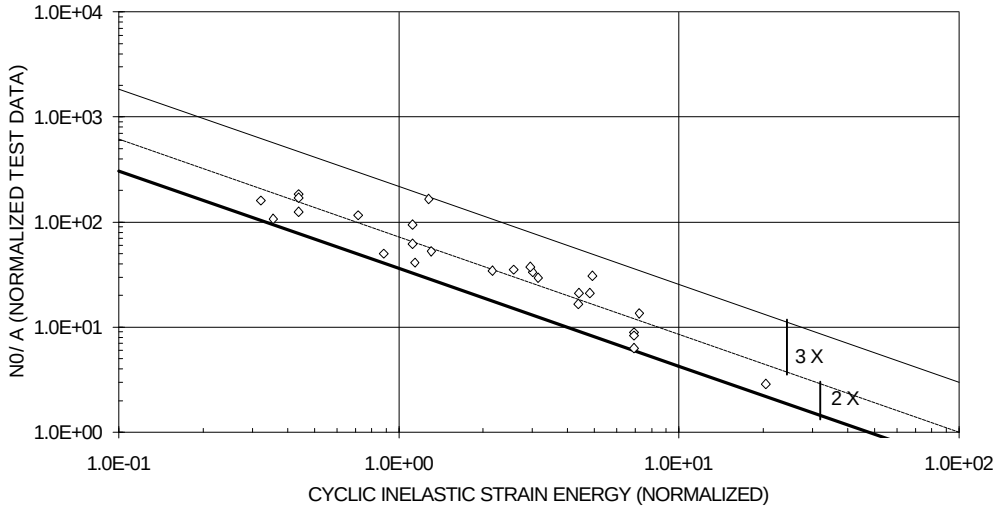

Figure 11: Correlation of Failure-Free Times Scaled for Solder Crack Areas versus Cyclic Inelastic Strain Energy.

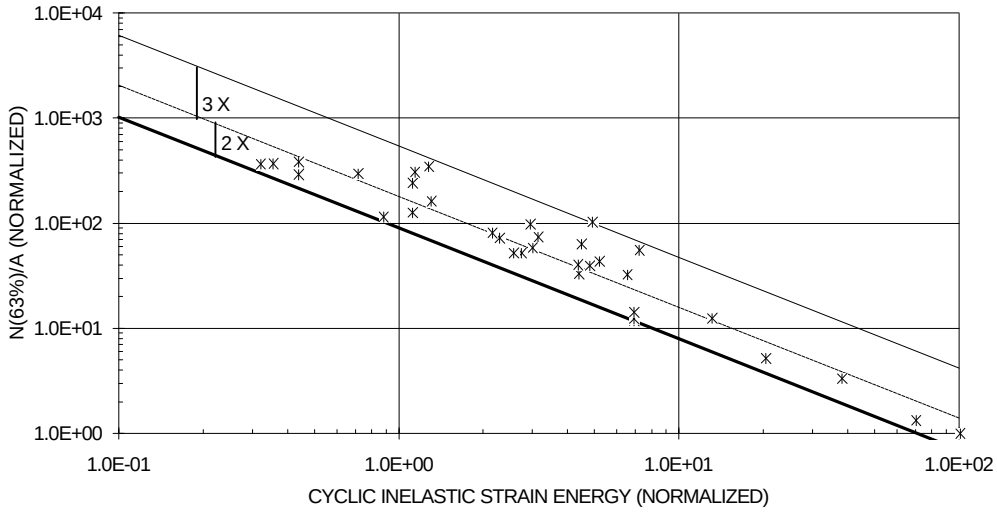

Figure 12: Correlation of Characteristic Lives Scaled for Solder Crack Areas versus Cyclic Inelastic Strain Energy.

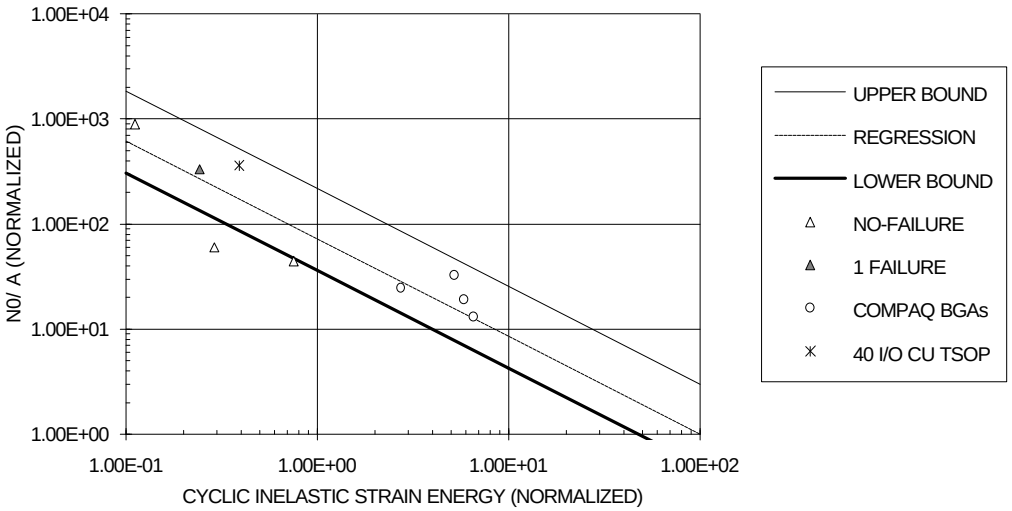

Figure 13: Fit of Additional Data to the Correlation of Failure-Free Times Scaled for Solder Crack Areas versus Cyclic Inelastic Strain Energy.

Additional data that fit or support the failure-free time correlation are shown in Figure 13:

- Four tests have zero or one failure. The N_0 estimates for these four tests are lower bounds shown as triangles. The N_0 lower bound estimates are obtained by setting the median rank CDF to F = (1-0.3)/(n+0.4) for the first failure (see footnote no. 3) and solving the 3P Weibull CDF equation for N_0:

$$\frac{0.7}{n+0.4} = 1 - \exp[-(\frac{N^* - N_0}{\alpha - N_0})^\beta] \qquad (4)$$

  where n is the sample size and β = 2.2. The parameter α is estimated from the lower bound of the CSMR characteristic life correlation and N^* is the number of cycles to the first and only failure for the tests with one failure or the number of cycles at end of test plus one for the three tests that did not have any failure. For the latter, we assume that the first failure would have occurred at the next cycle had the test been continued. The lower bound estimates of N_0/A support the failure-free time correlation since the data fall within or below the correlation band.

- The COMPAQ Ball Grid Array (BGA) data, shown as circles, are from accelerated tests where the characteristic lives, α_{test}, and cycles to first failure, N_{1st} , were reported in [42]. Since failure logs were not available, N_0 was obtained by solving the median-rank CDF equation at the time the first failure occurred:

$$\frac{0.7}{n+0.4} = 1 - \exp[-(\frac{N_{1st} - N_0}{\alpha_{test} - N_0})^\beta] \qquad (5)$$

  The COMPAQ data fit the failure-free time correlation band.

- The 40 I/O copper TSOP [43] data point, shown as a star, had failure statistics available for Weibull analysis and also fits the failure-free time model.

The validity of the failure-free time and characteristic life correlations will be further tested as new thermal cycling data with failure logs become available.

The N_0/A and α/A cyclic lives scaled for the solder crack area are interpreted as parameters of a distribution of inverted crack propagation rates. N_0/A gives the fastest rate for growing cracks and producing an open through the weakest joint of the population being assessed. Figure 14 shows the regression lines for the N_0/A and α/A (=N(63.2%)/A) data versus cyclic strain energy

as well as inverted crack propagation rates (dN/dA) from measurements by R. Darveaux. [21] The crack area propagation rates (dA/dN) were obtained from crack length and crack area measurements averaged over 3 devices x 8 corner joints/device = 24 joints every time devices were pulled out of test. The mean dN/dA vs. ΔW_{in} relationship for 60Sn-40Pb has a slope of -0.971 [21] very close to the slopes of our N_0/A and α/A regression lines. Considering that crack initiation is a small fraction of the fatigue live [21, 33], Darveaux's dN/dA line for mean crack propagation rates is remarkably close to our regression line for characteristic lives and supports the above interpretation of N_0/A and α/A in terms of crack propagation rates.

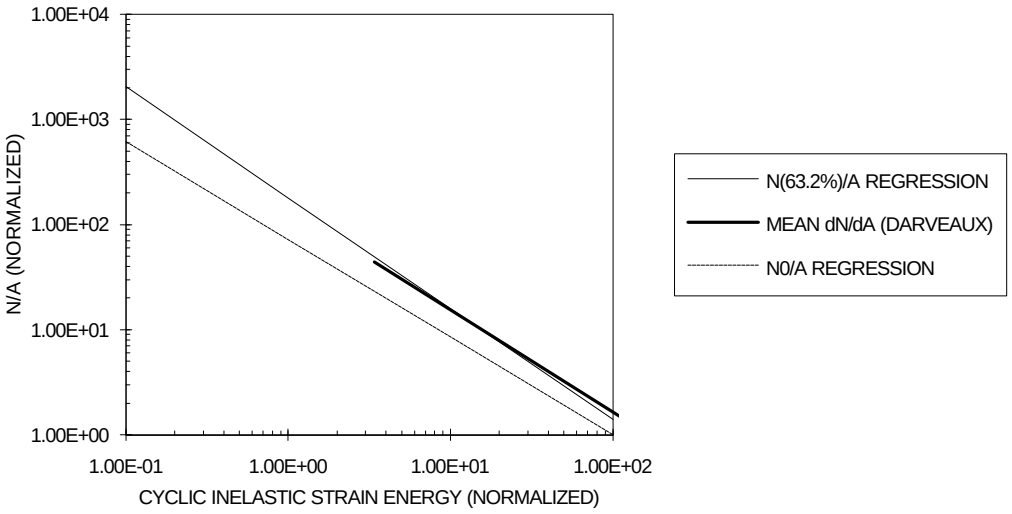

Figure 14: Comparison of R. Darveaux's Crack Propagation Data [21] and CSMR Regressions of Characteristic Lives and Failure-Free Times Scaled for Solder Crack Areas.

APPLICATIONS

Design-For-Reliability Rules

For a given component assembly and anticipated use conditions, reliability goals are stated in terms of failure-free life, N_0, or acceptable cumulative failure distribution, F, at the end of the design life (N cycles of operations for a single thermal load):

- When $N < N_0$ or $D_0 = \frac{N}{N_0} < 1$, no wear-out failures are expected in service. The number of cycles of operation N is specified in the product design requirements and N_0 is estimated from the CSMR model. The failure-free cumulative damage D_0 represents the fraction of available failure-free time that has been used up at the end of the design life.
- When $N > N_0$ and $N < N_f(F)$, or $D_f(F) = \frac{N}{N_f(F)} < 1$, reliability requirements are met but the cycles of operation exceed the failure-free time. $N_f(F)$ is the number of service cycles to the acceptable proportion failed F. The cumulative fatigue damage $D_f(F)$ represents the fraction of available fatigue life or cycles to the acceptable failure level F that has been used up at the end of the design life.
- When $N > N_f(F)$, or $D_f(F) = \frac{N}{N_f(F)} > 1$, reliability goals are not met. Accelerated testing is recommended when the reliability goals are not met marginally, i.e. when $D_f(F)$ is slightly larger than 1.

Similar rules apply when the product thermal history includes multiple thermal loads encountered in Environmental Stress Testing (EST), storage and transport, or when service conditions include severe or worst case thermal cycles. The cumulative failure-free damage D_0 and the cumulative fatigue damage $D_f(F)$ are then estimated using Miner's rule [44]:

$$D_0 = \sum_i \frac{N_i}{N_{0,i}} < 1 \qquad (6)$$

$$D_f(F) = \sum_i \frac{N_i}{N_{f,i}(F)} < 1 \qquad (7)$$

where N_i is the number of cycles for each thermal load (index i). $N_{0,i}$ is the failure-free time and $N_{f,i}(F)$ is the cycles to a proportion failed F for each thermal condition i. Miner's rule, originally derived from cumulative strain energy considerations, has not been formally validated for solder joint failures. We believe that Miner's rule applies to solder joint fatigue since the CSMR database correlations of failure-free times and characteristic lives are also energy based.

Design Examples

Example 1: Failure-Free Life Prediction.

The assembly is a PolyHIC [45] module on FR-4 (CTE = 18 ppm/^{o}C) for hypothetical use in an outdoor cabinet with a 20 year design life requirement. The hypothetical thermal history includes EST, storage and transport cycles and a daily thermal cycle (365.25 cycles/year) between 35^{o}C and 70^{o}C in operation. The temperature swings, dwell times and number of cycles for each condition are in Table 1.

CONDITION	T_{min} (^{o}C)	T_{max} (^{o}C)	Dwell (minutes)	N_i (cycles)	$N_{0,i}$ (cycles)	Damage: $N_i/N_{0,i}$
1. EST	-20	70	30	20	2980	0.67%
2. STORAGE	-20	25	720	25	11707	0.21%
3. TRANSPORT	-40	25	720	25	5296	0.47%
4. OPERATION	35	70	720	20 x 365.25 = 7305	14241	51.30%
						D_0 = 52.65%

Table 1: PolyHIC Thermal Conditions and Cumulative Failure-Free Damage at 20 years.

The failure-free cycles $N_{0,i}$ for each thermal condition are based on the lower bound of the CSMR correlation of failure-free times. The cumulative damage D_0 = 52.65 % is less than 1, thus the PolyHIC SM assembly is failure-free beyond the specified design life of 20 years. Note also that the pre-service cycles (EST, storage and transport) only have a small contribution to the cumulative damage at 20 years. The maximum possible failure-free time N_0(years) is obtained by setting Miner's cumulative damage for failure-free times equal to 1 and solving for N_0(years), i.e.:

$$\sum_{i=1}^{4} \frac{N_i}{N_{0,i}} = 1 \text{ , or: } \frac{20}{2980} + \frac{25}{11707} + \frac{25}{5296} + \frac{365.25 \times N_0(\text{years})}{14241} = 1 \qquad (8)$$

from which we get: N_0(years) = 38.46 years. The actual failure-free life exceeds the design life by a factor: 38.46 years / 20 years = 1.92. The 20 year failure-free life is thus met with a large "safety" margin since, in addition to this 1.92 factor, predictions are based on the lower bound of the CSMR database correlation.

Example 2: Failure-Free Life Prediction and Cumulative Distribution of Failures.

The assembly is code 1206 discrete resistors (CTE = 6 ppm/^{o}C) on FR-4 (CTE = 18 ppm/^{o}C) with a 20 years design life in an outdoor cabinet environment. The hypothetical product thermal history includes EST, storage and transport cycles and a daily thermal cycle (365.25 cycles/year) between 35^{o}C and 70^{o}C in operation. The temperature swings, dwell times and number of cycles for each condition and a 20 year design life are in Table 2.

CONDITION	T_{min} (^{o}C)	T_{max} (^{o}C)	Dwell (minutes)	N_i (cycles)	$N_{0,i}$ (cycles)	Damage: $N_i/N_{0,i}$
1. EST	-20	70	30	20	1553	1.29%
2. STORAGE	-20	25	720	25	4422	0.57%
3. TRANSPORT	-40	25	720	25	2307	1.08%
4. OPERATION	35	70	720	20 x 365.25 = 7305	7760	94.13%
						D_0 = 97.07%

Table 2: "1206s" Thermal Conditions and Cumulative Failure-Free Damage at 20 years.

The cumulative failure-free damage at 20 years is D_0 = 97.07%, slightly less than 1. The 20 year failure-free life requirement is met and the maximum expected failure-free life is 20.62 years (obtained by setting D_0 = 1). The "safety" margin is low, however, the results are conservative since predictions are based on the lower bound of the failure-free time correlation and test data for resistors are above the central regression line of the correlation band, that is, at least a factor of 2 above the lower bound.

The wear-out failure distribution starts at 20.62 years. Table 3 shows that the cumulative wear-out damage $D_f(F)$ for a targeted proportion failed F = 0.02% at 25 years is larger than 1.

CONDITION	T_{min} (^{o}C)	T_{max} (^{o}C)	Dwell (minutes)	N_i (cycles)	$N_{f,i}$ (cycles)	Damage: $N_i/N_{f,i}$
1. EST	-20	70	30	20	1583	1.26%
2. STORAGE	-20	25	720	25	4534	0.55%
3. TRANSPORT	-40	25	720	25	2357	1.06%
4. OPERATION	35	70	720	25 x 365.25 = 9131.25	7983	114.38%
						$D_f(F)$ = 117.25%

Table 3: "1206s" Thermal Conditions and Cumulative Wear-Out Damage at 25 years.

The actual CDF at 25 years is solved for by setting $D_f(F)$ equal to 1 in Equation (7). We find F = 1.52%. The plot of the CDF versus time in Figure 15 shows that the cumulative proportion failed increases rapidly after the failure-free life has been exceeded.

Figure 15: CDF versus Service Life for 1206 Resistors in Outdoors Cabinet (Example 2).

Other Applications:

Failure-free time estimates for other assemblies are shown in Table 4 in perspective with predictions based on 2P Weibull projections. The thermal history is a daily cycle between 35^{o}C and 70^{o}C for a design life of 20 years. The common substrate CTE is 18 ppm/^{o}C. Failure-free time predictions are based on the lower bound of the CSMR correlation.

COMPONENT	FAILURE-FREE LIFE (YEARS)	CUMULATIVE PPM @ 20 YEARS 2P WEIBULL PROJECTIONS
1206 RESISTOR	20.6	275
SOT-23	37	120
POLYHIC	39	194
132 I/O PQFP	83	5

Table 4: Comparison of Failure-Free Times and Cumulative CDF Predictions (in ppm) from 2P Weibull Analysis.

The 1206 resistors had a CDF of 275 ppm at 20 years based on 2P Weibull analysis whereas the 3P Weibull analysis is failure-free beyond the 20 year design life. The reliability gain is more obvious for the other devices where the failure-free life from 3P Weibull is much larger than 20 years. While the SOT-23 and PolyHIC assemblies had acceptable CDFs between 100 and 200 ppm at 20 years, the failure-free analysis gives failure-free times of 37 and 39 years, respectively. This is a significant gain which, for other devices and use environments, translates into meeting reliability requirements based on 3P Weibull analysis or not passing the requirements based on 2P Weibull. The 83 year failure-free life for the 132 I/O PQFP exceeds the 20 year design life requirement by a large margin.

Test Data Extrapolation

As a result of the linear acceleration property of life test data (see Appendix), the 3P Weibull shape parameters are identical for test and field conditions and the failure-free times and characteristic lives have the same acceleration factor, i.e.:

$$\beta_{field} = \beta_{test} = \beta \quad (9)$$

$$\alpha_{field} = AF \times \alpha_{test} \quad (10)$$

$$N_{0,field} = AF \times N_{0,test} \quad (11)$$

$N_{0,test}$, α_{test} and β are given by the 3P Weibull analysis of the test data. The acceleration factor AF is obtained from the cyclic inelastic strain energies: $\Delta W_{in,test}$ and $\Delta W_{in,field}$ for test and field conditions, respectively:

$$AF = \left(\frac{\Delta W_{in,test}}{\Delta W_{in,field}}\right)^{p} \quad (12)$$

where the exponent p is close to 1. Since the slopes of the median regression lines for the N_0/A and α/A correlations are slightly different (-1.05 vs. -0.93; see Figure 14) we use the smaller value p = 0.93 from the N_0/A correlation. This value of p is slightly less than the 0.971 exponent of Darveaux's crack propagation rate equation and is thought to give conservative estimates of AFs.

For N cycles of a given thermal cycle in the field, wear-out failures are not expected up to $N = N_{0,field} = AF \times N_{0,test}$. For $N > N_{0,field}$, the cumulative distribution of failures or proportion failed at cycle N is:

$$F_{field}(N) = 1 - \exp\left[-\left(\frac{N - AF \times N_{0,test}}{AF \times \alpha_{test} - AF \times N_{0,test}}\right)^{\beta}\right] \quad (13)$$

Example 3: Alloy 42 Leaded TSOPs (2 Meg devices) and Copper Leaded TSOPs (die-up).

The failure-free test data is for 32 I/O 2Meg Alloy42 leaded TSOPs (RUN 2B in [8]; CTE = 19.6 ppm/^{o}C for the test boards) and 32 I/O 2Meg copper leaded TSOPs (die-up configuration in [46]; CTE = 19 ppm/^{o}C for the test boards). Acceleration factors are calculated for a circuit-board CTE of 18 ppm/^{o}C and an outdoor cabinet use environment characterized by a daily thermal cycle between 35^{o}C and 70^{o}C. Results are shown in Table 5 in perspective with failure rate predictions based on 2P Weibull projections.

TSOP	$N_{0,test}$ (cycles)	AF	$N_{0,field}$ (cycles)	$N_{0,field}$ (years)	Cum. ppm @ 10 Years 2P Weibull Projections
Alloy 42	767	3.28	2515	6.9	880000 (= 88%)
Copper	2800	4.38	12264	33.5	52000 (= 5.2%)

Table 5: Extrapolated Failure-Free Times and Cumulative CDF Predictions (in ppm) at 10 years from 2P Weibull Analysis.

The ratio of failure-free lives for the copper and Alloy 42 configurations is: 33.5 / 6.9 = 4.85, consistent with previous conclusions [46] that solder joints of copper leaded TSOPs on FR-4 have a fatigue live about five times larger than solder joints of Alloy 42 TSOPs.

The projected failure-free life in the field is 33.5 years for the copper TSOP example. A 20 year design life requirement would be met with a "safety" margin of 33.5 / 20 = 1.675. The failure-free projection of more than 20 years is a significant gain over the projected 5.2% cumulative failure at 10 years from the 2P Weibull analysis of the data [46].

For Alloy 42 TSOPs, the projected failure-free life is 6.9 years in the field consistent with the 5 year service life restriction for telecommunication applications [8]. From the 3P Weibull analysis of test data: α_{test} = 1918, β = 2.287 and the predicted CDF at 10 years (N = 10 x 365 = 3650 cycles) is:

$$F_{field}(10\ \text{years}) = 1 - \exp[-(\frac{3650 - 3.28 \times 767}{3.28 \times 1918 - 3.28 \times 767})^{2.287}] = 6.2\%$$

also a significant gain compared to the 88% cumulative failure projection from 2P Weibull analysis [46].

CONCLUSIONS

The 3P Weibull treatment of SM assembly failure data enhances the CSMR design tool by enabling the prediction of failure-free times for assembly reliability. The 3P Weibull analysis is supported by a large test database and further exploits failure statistics at the tail end of solder joint failure distributions. In general, we expect better and more accurate reliability projections than were made in the past based on conservative 2P Weibull analysis.

ACKNOWLEDGMENTS

Many thanks to J. A. Augis and L. L. Hines for resurrecting old failure data and lab notebooks. We also thank T. I. Ejim for the 40 I/O Cu TSOP data, and J. S. Erich, P. M. Hall and W. M. Sherry for the legacy of their bicycle chain lab notebook. Last, we would like to acknowledge the many individuals and organizations who over the years have contributed in different ways to the development of the test database without which this work would have been impossible. Special thanks to T. M. Lach, P. C. Moy and G. C. Munie for their strong support and encouragement, and J. A. Augis and R. L. Shook for their review of this paper.

REFERENCES

[1] W. Weibull, "A Statistical Distribution Function of Wide Applicability," *Journal of Applied Mechanics*, September 1951, pp. 293-297.

[2] R. B. Abernethy, J. E. Breneman, C. H. Medlin and G. L. Reinman, *Weibull Analysis Handbook*, Air Force Wright Aeronautical Laboratories, National Technical Information Service, November 1983.

[3] R. B. Abernethy, *The New Weibull Handbook*, Publisher: R. B. Abernethy, North Palm Beach, FL, October 1993.

[4] P. D. T. O'Connor, *Practical Reliability Engineering*, 2nd Edition, John Wiley & Sons, 1989, pp. 36-45 and 71-79.

[5] *A Guide for Fatigue Testing and the Statistical Analysis of Fatigue Data*, ASTM Special Technical Publication No. 91-A (2nd edition), ASTM, Philadelphia, PA, 1963, pp. 71-79.

[6] P. A. Tobias and D. Trindade, *Applied Reliability*, Van Nostrand Reinhold, 1986.

[7] J-P. Clech, J. C. Manock, D. M. Noctor, F. E. Bader and J. A. Augis, "A Comprehensive Surface Mount Reliability (CSMR) Model Covering Several Generations of Packaging and Assembly Technology," Proceedings, 43rd ECTC, Orlando, FL, June 1-4, 1993, pp. 62-70.

[8] D. M. Noctor, F. E. Bader, A. P. Viera, P. Boysan, S. Golwalker and D. Foehringer, "Attachment Reliability Evaluation and Failure Analysis of Thin Small Outline Packages (TSOPs)," Proceedings, 43rd ECTC, Orlando, FL, June 1-4, 1993, pp. 54-61.

[9] "Guidelines for Accelerated Reliability Testing of Surface Mount Solder Attachments," IPC-SM-785, Institute for Interconnecting and Packaging Electronic Circuits, Lincolnwood, IL, November 1992.

[10] NASA Handbook, NHB 5300.4 (3A-1).

[11] R. Iannuzzelli, "Predicting Solder Joint Reliability, Model Validation," Proceedings, 43rd ECTC, Orlando, FL, June 1-4, 1993, pp. 839-851.

[12] J. Seyyedi and S. Jawaid, "Wear-out Evaluation of Soldered Interconnections for Surface Mounted Leadless and Leaded Components," *Soldering and Surface Mount Technology*, No. 4, February 1990, pp. 44-49.

[13] T. P. Parker, C. W. Webb, "A Study of Failures Identified During Board Level Environmental Stress Testing," Proceedings, 42nd ECTC, San Diego, CA, May 1992, pp. 177-184.

[14] D. M. Noctor, C. W. Glessner and G. W. Lynott, AT&T Bell Laboratories, unpublished data, 1991.

[15] L. S. Goldmann, "Geometric Optimization of Controlled Collapse Interconnections," *IBM Journal of Research and Development*, May 1969, pp. 251-265.

[16] K. C. Norris and A. H. Landzberg, "Reliability of Controlled Collapse Interconnections," *IBM Journal of Research and Development*, May 1969, pp. 266-271.

[17] B. Wong and D. E. Helling, "A Mechanistic Model for Solder Joint Failure Prediction Under Thermal Cycling," *Transactions of the ASME, Journal of Electronic Packaging*, December 1990, Vol. 112, pp. 104-112.

[18] A. Dasgupta, C. Oyan, D. Barker and M. Pecht, "Solder Creep-Fatigue Analysis by an Energy Partitioning Approach," *Transactions of the ASME, Journal of Electronic Packaging*, June 1992, Vol. 114, pp. 152-160.

[19] J. Sauber and J. Seyyedi, "Predicting Thermal Fatigue Lifetimes for SMT Solder Joints," *Transactions of the ASME, Journal of Electronic Packaging*, December 1992, Vol. 114, pp. 472-476.

[20] Y-H. Pao, R. Govila, S. Badgley and E. Jih, "An Experimental and Finite Element Study of Thermal Fatigue Fracture of PbSn Solder Joints," *Transactions of the ASME, Journal of Electronic Packaging*, March 1993, Vol. 115, pp. 1-8.

[21] R. Darveaux, "Crack Initiation and Growth in Surface Mount Solder Joints," Proceedings, ISHM Conference, November 9-11, 1993, Dallas, TX, pp. 86-97.

[22] P. M. Hall und W. M. Sherry, "Materials, Structures and Mechanics of Solder-Joints for Surface-Mount Microelectronics Technology," Verbidungstechnik in der Electronic, Deutsche Verband für Schweißtechnick, 3rd International Conference, Fellbach, West Germany, February 18-20, 1986, pp. 47-61.

[23] J. S. Erich, P. M. Hall and W. M. Sherry, AT&T Bell Laboratories, lab notebook, 1984.

[24] T. Caulfield, J. A. Benenati and J. Acocella, "Surface Mount Array Interconnections for High I/O MCM-C to Card Assemblies," Proceedings, ICEMM '93, pp. 320-325.

[25] J. C. Manock, AT&T Bell Laboratories, unpublished data, 1993.

[26] L. L. Hines, "SOT-23 Surface Mount Attachment Reliability Study," Proceedings, IEPS Conference, Boston, MA, November 9-11, 1987, pp. 613-629. Also in 52415-870901-11TM.

[27] E. Nicewarner, "Effect of Solder Joint Geometry and Conformal Coating on Surface Mount Solder Joint Fatigue Life," Proceedings, Nepcon East '93, Boston, MA, June 15-17, 1993, pp. 207-216.

[28] E. Nicewarner, "Historical Failure Distribution and Significant Factors Affecting Surface Mount Solder Joint Fatigue Life," Proceedings, IEPS '93, San Diego, CA, September 12-15, 1993, pp. 553-563.

[29] F. R. Nash, *Estimating Device Reliability: Assessment of Credibility*, Kluwer Academic Publishers, 1993, Chapter 7, pp. 123-161.

[30] G. Dieter, *Engineering Design*, McGraw-Hill, 1983, pp. 391-394.

[31] C. H. Lipson and N. J. Seth, *Statistical Design and Analysis of Engineering Experiments*, McGraw-Hill, 1973, pp. 175-181.

[32] C. S. Yen, "Fatigue Statistical Analysis", in *Metal Fatigue: Theory and Design*, ed. A. F Madayag, J. Wiley & Sons, 1969, Chapter 5, pp. 140-169.

[33] Mitsubishi paper, ASME Binghamton, September 1993 (PQFP crack propagation data).

[34] J. Seyyedi, "Thermal Fatigue Behaviour of Low Melting Point Solder Joints," *Soldering and Surface Mount Technology*, No. 13, February 1993, pp. 26-32.

[35] J. W. Morris, Jr., D. Tribula, T. S. E. Summers and D. Grivas, "The Role of Microstructure in Thermal Fatigue of Pb-Sn Solder Joints," in *Solder Joint Reliability: Theory and Applications*, ed. J. H. Lau, Van Nostrand Reinhold, 1990, pp. 225-265.

[36] D. R. Frear, "Thermomechanical Fatigue in Solder Materials," in *Solder Mechanics: A State of the Art Assessment*, Santa Fe, NM, June 1990, ed. D. R. Frear, W. B. Jones and K. R. Kinsman, TMS (The Minerals, Metals & Materials Society), 1991, pp. 191-237.

[37] D. Frear, D. Grivas and J. W. Morris, Jr., "Parameters Affecting Thermal Fatigue Behavior of 60Sn-40Pb Solder Joints," *Journal of Electronic Materials*, Vol. 18, No. 6, 1989, pp. 671-680.

[38] D. Frear, D. Grivas and J. W. Morris, Jr., "A Microstructural Study of the Thermal Fatigue Failures of 60Sn-40Pb Solder Joints," *Journal of Electronic Materials*, Vol. 17, No. 2, 1988, pp. 171-180.

[39] H. D. Solomon, "Predicting Thermal and Mechanical Fatigue Lives from Isothermal Low Cycle Data", in *Solder Joint Reliability: Theory and Applications*, ed. J. H. Lau, Van Nostrand Reinhold, 1990, pp. 406-454.

[40] R. B. Abernethy, Consultant, North Palm Beach, FL, private communication, December 2, 1993.

[41] C. R. Mischke, "Rolling Contact Bearings," Chapter 7, *Standard Handbook of Machine Design*, eds. J. E. Shigley and C. R. Mischke, McGraw-Hill, 1986, pp. 27.1-27.17

[42] R. Johnson, A. Mawer, T. McGuiggan, B. Nelson, M. Petrucci and D. Rosckes, "A Feasibility Study of Ball Grid Array Packaging," Proceedings, Nepcon East '93, Boston, MA, June 14-17, 1993, pp. 413-422; also presented at Surface Mount International Conference, San-Jose, CA, August 29-September 2, 1993.

[43] T. I. Ejim, AT&T Bell Laboratories, unpublished data, 1993.

[44] M. A. Miner, "Cumulative Fatigue Damage," *Journal of Applied Mechanics*, September 1945, pp. A-159-A-184.

[45] J. C. Manock and P. C. Moy, "Solder Joint Reliability and Failure Analysis of the 244 I/O Pre-Molded PolyHIC Package," Proceedings, 43rd ECTC, Orlando, Florida, June 1-4, 1993, pp. 1156-1160. Also in 103216000-930506-01TM.

[46] D. M. Noctor and J-P. Clech, "Accelerated Testing and Predictive Modeling of the Attachment Reliability of Alloy 42 and Copper Leaded TSOPs," Proceedings, Nepcon East '93, Boston, MA, June 14-17, 1993, pp. 193-206. Also in 536150000-930322-01TM.

APPENDIX: 3P WEIBULL EQUATIONS AND PROPERTIES

Cumulative Distribution Function:

for $N < N_0$: $F(N) = 0$

for $N > N_0$: $$F(N) = 1 - \exp[-(\frac{N - N_0}{\alpha - N_0})^{\beta}] \quad (A.1)$$

where the characteristic life, α, and the minimum life or failure-free time, N_0, are obtained from accelerated test data or calculated with the CSMR model. An average value of the shape parameter β for SM assembly 3P Weibull distributions is $\beta = 2.2$.

For $N = \alpha$, the CDF is $F = 1 - 1/e \approx 63.2\%$ independently of N_0 and β.

The cycle count to a CDF of F is: $$N = N_0 + (\alpha - N_0) \times [-\ln(1 - F)]^{1/\beta} \quad (A.2)$$

Reliability Function: $$R(N) = 1 - F(N) \quad (A.3)$$

Hazard Rate Function (Instantaneous Failure Rate) for $N > N_0$:

$$h(N) = \frac{\beta(N - N_0)^{\beta - 1}}{(\alpha - N_0)^{\beta}} = \frac{\beta}{N - N_0}(\frac{N - N_0}{\alpha - N_0})^{\beta} \quad (A.4)$$

A useful expression for h(N) as a function of the CDF is:

$$h(N) = \frac{\beta}{N - N_0}[-\ln(1 - F(N))] \quad (A.5)$$

h(N) has units of failures per unit of time (or per cycle when N is the number of cycles)

For N and N_0 in hours, the instantaneous failure rate in FITs (failures in 10^9 hours) is:

$$\text{iFITs} = h(N) \times 10^9 \tag{A.6}$$

$$\text{iFITs} = \frac{\beta \times 10^9}{N - N_0}[-\ln(1 - F(N))] \tag{A.7}$$

Acceleration Factor for the 3P Weibull Distribution

As a result of linear acceleration, the 3P Weibull shape parameters are identical for test and field conditions and the failure-free times and characteristic lives have the same acceleration factor, i.e.:

$$\beta_{field} = \beta_{test} \tag{A.8}$$

$$\alpha_{field} = AF \times \alpha_{test} \tag{A.9}$$

$$N_{0,field} = AF \times N_{0,test} \tag{A.10}$$

This is demonstrated below. There is a similar derivation of this for 2P Weibull distributions in Tobias and Trindade (pp. 130-131), Reference 6 in the text.

The linear acceleration equation for all cycles N in the field is:

$$F_{field}(N) = F_{test}\left(\frac{N}{AF}\right) \tag{A.11}$$

By substituting the 3P Weibull distributions into (A.11), we get:

$$1 - \exp\left[-\left(\frac{N - N_{0,field}}{\alpha_{field} - N_{0,field}}\right)^{\beta_{field}}\right] = 1 - \exp\left[-\left(\frac{N/AF - N_{0,test}}{\alpha_{test} - N_{0,test}}\right)^{\beta_{test}}\right] \tag{A.12}$$

that is:

$$\left(\frac{N - N_{0,field}}{\alpha_{field} - N_{0,field}}\right)^{\beta_{field}} = \left(\frac{N - AF \times N_{0,test}}{AF \times \alpha_{test} - AF \times N_{0,test}}\right)^{\beta_{test}} \tag{A.13}$$

Equation (A.13) which must hold for all N larger than the failure-free times implies: $\beta_{field} = \beta_{test}$

Equation (A.13) then becomes:

$$\frac{N - N_{0,field}}{\alpha_{field} - N_{0,field}} = \frac{N - AF \times N_{0,test}}{AF \times \alpha_{test} - AF \times N_{0,test}} \tag{A.14}$$

Equation (A.14) must hold for all values of N, thus: $N_{0,field} = AF \times N_{0,test}$ and $\alpha_{field} = AF \times \alpha_{test}$.

As discussed in Tobias and Trindade [6] for 2P Weibull distributions, and contrary to popular belief, the equality of shape parameters is not an assumption, it is a consequence of the linear acceleration model.

Relationship between the Weibull Parameters of Component and Subset Failure Distributions

Failure data are acquired on a component basis or on a component sub-set basis. The first solder joint failure on a given component gives the time to failure of that component. While the other solder joints of a component will fail at a later time, the distribution of first component

failures is what we are interested in. On occasion, failure data are acquired with higher resolution than at the component level and the component is divided into k sub-sets. For example, since the PolyHIC data [45] was on an octile basis, k = 8 for 8 octiles per PolyHIC. If the size of the component population is n, the size of the sub-set population is k x n. In the PolyHIC experiment, the component population had a sample size of 32 components and the octile population had a sample size of 8 x 32 = 256 octiles. The component and the octile populations are two distinct populations with different failure distributions (see Figure A.1). As shown below, there is a mathematical relationship between the two failure distributions.

When the k subsets of a component are statistically and mechanically independent, the attachment of that component does not fail if none of the k sub-sets fails. Thus, the probability of non-failure of a component is:

$$1 - F_{component}(N) = (1 - F_{sub}(N))^k \tag{A.15}$$

for all cycles N.

The component Weibull distribution has parameters: $N_{0,comp}$, α_{comp} and β_{comp} and its CDF function is:

$$F_{comp}(N) = 1 - \exp[-(\frac{N - N_{0,comp}}{\alpha^*_{comp}})^{\beta_{comp}}] \tag{A.16}$$

where: $\alpha^*_{comp} = \alpha_{comp} - N_{0,comp}$.

The component subset Weibull distribution has parameters: $N_{0,sub}$, α_{sub} and β_{sub} and its CDF function is:

$$F_{sub}(N) = 1 - \exp[-(\frac{N - N_{0,sub}}{\alpha^*_{sub}})^{\beta_{sub}}] \tag{A.17}$$

where: $\alpha^*_{sub} = \alpha_{sub} - N_{0,sub}$.

By substituting the CDF functions into equation (A.15) we get:

$$(\frac{N - N_{0,comp}}{\alpha^*_{comp}})^{\beta_{comp}} = k \times (\frac{N - N_{0,sub}}{\alpha^*_{sub}})^{\beta_{sub}} \tag{A.18}$$

Equation (A.18) holds for all N larger than the failure-free times and implies: $\beta_{comp} = \beta_{sub} = \beta$. Equation (A.18) then becomes:

$$\frac{N - N_{0,comp}}{\alpha^*_{comp}} = \frac{N - N_{0,sub}}{\frac{\alpha^*_{sub}}{k^{1/\beta}}} \tag{A.19}$$

Equation (A.19) must hold for all cycles N larger than the failure-free times, thus:

$$N_{0,comp} = N_{0,sub} \tag{A.20}$$

and:

$$\alpha^*_{comp} = \frac{\alpha^*_{sub}}{k^{1/\beta}} \tag{A.21}$$

The physical interpretation of equal β's is that shape parameters reflect the spread of solder joint quality which is expected to be the same for the component sub-set population and for the component population, provided that all test vehicles come from the same batch. The equality of failure-free times is intuitively obvious. An example of data supporting equations (A.20) and (A.21) is given below.

The PolyHIC data was analyzed on a per component and per octile basis. Assuming that failures for the eight octiles of a component are independent, that is, the stress distributions on the solder joints of an octile are not affected by failed solder joints on other octiles of the same component,

the 3P Weibull analysis should give the same N_0 for the octile ("oct") and the component ("comp") populations. The relationship between the shifted characteristic lives is:

$$\alpha^*_{comp} = \frac{\alpha^*_{oct}}{8^{1/\beta}} \qquad (A.22)$$

where the shifted characteristic lives are the characteristic lives referred to the failure-free time origins: $\alpha^*_{comp} = \alpha_{comp} - N_{0,comp}$ and $\alpha^*_{oct} = \alpha_{oct} - N_{0,oct}$. The 3P Weibull parameters for PolyHIC octiles and component failures are tabulated below:

Population	N_0	α	α^*	β	$8^{1/\beta}$
Octiles	3091	18301	15210	2.956	2.02
Components	3768	10875	7107	2.334	2.44

The ratio of N_0's is: 3768/3091 = 1.22, that is, the N_0's are not quite equal as expected from the theory. The difference in N_0's is attributed to the statistical nature of the data and perhaps to the fact that the first failure stands slightly out of the failure distributions (see Figure A.1 below). The ratio of α^*'s is: 15210/7107 = 2.14 which is in the range of $8^{1/\beta}$ in the table above. To be on the conservative side when using the PolyHIC data in the CSMR correlations, we used the lowest value of N_0 = 3091 for the PolyHIC failure-free time and for the PolyHIC component characteristic life, we used the lowest value obtained from octile statistics and equation (A.22), that is:

$$\alpha_{comp} \approx N_{0,oct} + \frac{\alpha^*_{oct}}{8^{1/\beta_{oct}}} = 3091 + \frac{15210}{8^{1/2.956}} = 10617$$

which is slightly less than α_{comp} = 10875 obtained from component failure statistics. The relationship between the failure statistics of the component and octile populations is fairly good, suggesting that the failures of the 8 octiles of a given component are relatively independent of one another. The distinct failure distributions for the octile and component populations are shown on 2P Weibull paper in Figure A.1.

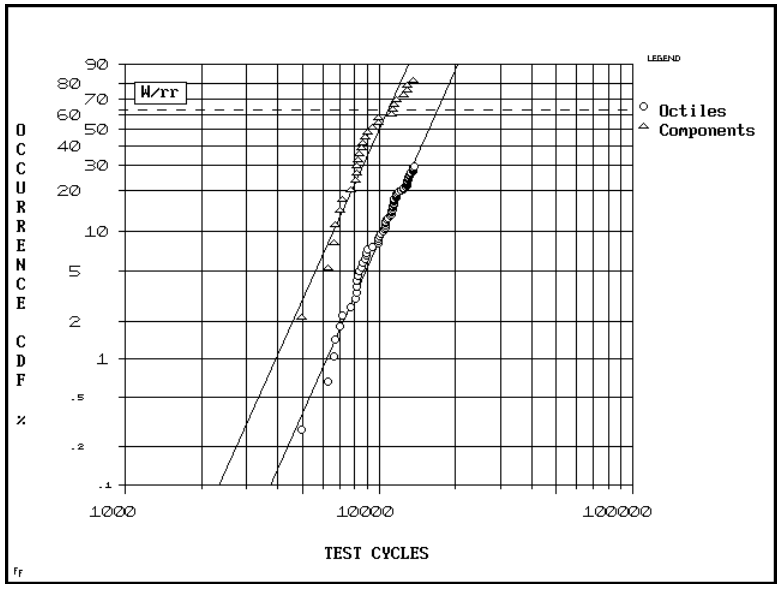

Figure A.1: PolyHIC component and octile failure distributions on 2P Weibull paper.